Available online at www.sciencedirect.com
SCIENCE DIRECT®
International Journal of Mass Spectrometry 233 (2004) 165–172
International Journal of Mass Spectrometry
www.elsevier.com/locate/ijms

Ionization energies of the C_{60} fullerene and its hydrogenated derivatives $C_{60}H_{18}$ and $C_{60}H_{36}$ determined by electron ionization

Andrey V. Pogulay [a], Rinat R. Abzalimov [a], Shamil' K. Nasibullaev [b], Anatoly S. Lobach [c], Thomas Drewello [d], Yury V. Vasil'ev [a,e,*]

[a] *Institute of Physics of Molecules and Crystals, Ufa Research Center of Russian Academy of Science, Ufa, Russia*
[b] *Bashkir State University, Ufa, Russia*
[c] *Institute of Problems of Chemical Physics, Russian Academy of Science, Chernogolovka, Moscow Region, Russia*
[d] *Department of Chemistry, University of Warwick, Coventry, UK*
[e] *Department of Physics, Bashkir State Agricultural University, Ufa, Russia*

Received 28 September 2003; accepted 21 December 2003

Dedicated to Professor Tilmann D. Märk on the occasion of his 60th birthday.

Abstract

Modification of a method for processing positive ion ionization efficiency curves of polyatomic molecules, as developed earlier by Märk and coworkers, has been described. Based on the method, the first, second, and third ionization energies of C_{60} have been re-examined and found to be in excellent agreement with the most reliable literature data. The ionization energies for $C_{60}H_{18}$ and $C_{60}H_{36}$ have been measured for the first time and were established as 7.3 ± 0.3 eV and 7.01 ± 0.25 eV, respectively. Although the appearance energy of $C_{60}H_{36}^{2+}$ (18.7 ± 0.2 eV) has been determined to be lower than that of C_{60}^{2+} (18.98 ± 0.35 eV), the reverse scenario is true for the second ionization energies of $C_{60}H_{36}$ and C_{60}.

Keywords: Ionization energy; Fullerenes; Hydrogenated fullerenes

1. Introduction

Ionization energies (first, second, etc.) are important thermodynamic characteristics of a molecule. The experimental determination of the vertical ionization energies is commonly based upon the measurement of the appearance energies of the corresponding positive ions (singly-, doubly-charged, etc.) as a function of the energy of ionizing radiation or particles. The appearance energies of positively-charged fullerenes were studied intensively over the last decade. In contrast to the vast majority of organic molecules for which ionization energies were determined by the different means of photoelectron spectroscopy, the ionization energies of the C_{60} fullerene have been studied equally thoroughly by electron ionization mass spectrometry employing state-of-the-art electron monochromators. The energy spread of the electron beam generated by the monochromators can be easily varied from several meV up to hundreds of meV depending on the desired ion signal intensity. The implementation of modern monochromator technology has paved the way for the "aged" technique of electron ionization to continue in modern uses of great fundamental importance. With respect to the energy resolution, mass spectrometry-based appearance energy measurements thus represents a major competition for modern photoelectron spectroscopy. Photo and electron ionization are characterized by a different ionization cross-section behavior near the threshold. The earliest studies of C_{60} by electron ionization already revealed that processing the ionization efficiency curve at threshold constitutes a most challenging task for the technique. It is generally recognized that the theoretical description of the atomic electron ionization cross-section near the threshold has been established by Wannier [1] for the case of the simple singly-charged atomic

* Corresponding author.
E-mail address: y.vasilev@orst.edu (Y.V. Vasil'ev).

1387-3806/$ – see front matter © 2004 Elsevier B.V. All rights reserved.
doi:10.1016/j.ijms.2003.12.016

ion H^+:

$$\sigma \propto E^p, \tag{1}$$

where E is electron energy and $p \approx 1.127$ is the Wannier exponent. Although there is no general theoretical consideration for the case of polyatomic molecules, it is believed that the same power laws hold true for each single ionic state of the molecule. Because a number of different electronic, vibrational, and rotational states may be present in a polyatomic molecule, its ionization cross-section becomes a complex function of electron energy even near the ionization threshold, E_1. As a result, the ionization efficiency curve may show a pronounced curvature near E_1 and the exponent p may well exceed z, the charge of the ion under study. This is particularly true in the case of fullerenes that possess an enormous density of states at typical temperatures applied to their efficient evaporation into the gas phase. Märk and coworkers was amongst the first to indicate this problem and contributed greatly to the determination of appearance energies of single- and multiple-charged parent [2,3] and fragment [4] ions produced from C_{60} and C_{70} by electron ionization mass spectrometry.

In earlier attempts to analyze the ionization efficiency curves of C_{60} and C_{70} [2,4], Märk and coworkers raised the original data points to a certain power ($1/p$), in order to linearize the lower part of the curves near the ionization onset. Surprisingly, this approach led especially in the case of multiply-charged ions to much lower appearance energies than those expected for a simple extrapolation of the linear-appearing part of the positive ion ionization efficiency curve. However, it was recognized later that such a procedure [3], leads to a slight systematic overestimation of p and E_1, which is associated with the issue of linearization and with prominent background contributions. To overcome the problem, Märk and coworkers [3,5] applied a weighted, non-linear least-squares fitting procedure to the raw data, using the Marquardt-Levenberg algorithm. The weights were chosen as $1/(N+1)$ where N is the total number of counts per energy bin. The fitting function was as follows [3,5]:

$$f(E) = \begin{cases} b & \text{if } E \leq E_1, \\ b + c(E - E_1)^p & \text{if } E > E_1, \end{cases} \tag{2}$$

where b stands for background and c is a fitting constant that depends on the particular instrument. The last refinement of the original data processing procedure is taking into account the convolution of the fitting function (2) with the electron energy distribution [6]. As instrumental function, Märk and coworkers used a Gaussian function [6].

The present paper details a modification of this approach and its application to multiple-charged fullerene ions of C_{60} and the hydrogenated derivatives $C_{60}H_{36}$ and $C_{60}H_{18}$. As mentioned above, the determination of ionization energies from ionization efficiency curves of C_{60} ions has employed a simple procedure whereby raising the original data points to a certain power ($1/p$) [2,4]. As far as the authors are aware, more sophisticated processing procedures have not been tested for the use with fullerene ions. It should also be emphasized that ionization energies of fullerene derivatives, with the exception of isolated $C_{60}F_{36}$ and $C_{60}F_{48}$ [7], and mixed $C_{60}F_{46,48}$ and $C_{70}F_{54,56}$ [8], have not been reported in the literature. Based on proton-transfer reactions, Compton and coworkers [9] predicted the ionization energies of $C_{60}H_x$ ($x = 2$–18) to be lower than 7.53 eV. However, difficulties associated with the thermal lability of the compounds during evaporation into vacuum prevented a more precise determination. In the present experiments, thermal decomposition was successfully prevented, allowing for the first time accurate measurements of ionization energies of hydrogenated fullerenes.

2. Experimental

The experiments have been performed with a single focusing magnetic sector mass spectrometer (MI 1201, Russia). The instrument [10] is equipped with a custom-built inlet system for thermally labile solids and a custom-built [11] trochoidal electron monochromator (TEM) [12] for the generation of a quasi-monoenergetic electron beam (full-width at half-maximum, FWHM, ΔE from 100 to 300 meV). The energy scale was calibrated using singly and doubly-charged positive Ar ions. In operation, the pressure measured with an ion gauge outside the ionization chamber did not exceed 10^{-7} Torr, which corresponds to single-collision conditions. The temperature of the oven, from which the samples were introduced into the ionization chamber, can be varied and was set to approximately 300 °C ($C_{60}H_{36}$), 350 °C ($C_{60}H_{18}$), and 450 °C (C_{60}). The samples were initially loaded into a glass capillary, which was then inserted into the oven. Capillary and oven had good thermal contact, so that similar temperatures could be assumed for both. To avoid direct contact of the samples under investigation with the metal surfaces (which usually serve as good catalysts for decomposition reactions of the fullerene derivatives), the tip of the capillary was positioned slightly outside the oven exit. Then the oven was introduced at the closest distance possible to the ionization chamber to achieve a high molecular density in the reaction zone. Since $C_{60}H_{18}$ and $C_{60}H_{36}$ are known to decompose very easily into C_{60} and fullerenes of lower hydrogen content [13], the abundance of the positive ions of C_{60} and neighboring hydrogen containing fullerene ions have been used as a measure to keep the possible decomposition of the samples under control. Usually, each sample loading allowed experiments to be conducted for approximately 1 h without dramatic decomposition of the samples. In this period, the intensity of the C_{60}^+ signal did not exceed 5% of the molecular ion signals $C_{60}H_{18/36}^+$, both being measured at an energy of 80 eV.

The C_{60} fullerene sample was purchased from Southern Chemical Group, LLC, (99.5% purity). $C_{60}H_{36}$ and $C_{60}H_{18}$ were synthesized by hydrogen transfer reduction

[14] from DHA (dihydroanthracene). Details of the synthesis have been published elsewhere [15]. The purity of the hydrogenated fullerene samples has been established by matrix-assisted laser desorption/ionization (MALDI) mass spectrometry [16].

3. Data analysis

The phenomenological model of the process of electron ionization as proposed in refs. [3,5,6] and based upon Eq. (2) considers the full ionization cross-section of a molecule as the sum of the partition contributions from separate channels:

$$\sigma(E) = \sum_i A_i \exp\{p_i \ln_0(E - E_i)\},$$

$$\text{where } \ln_0(E - E_i) = \begin{cases} E \le E_i: & -\infty \\ E > E_i: & \ln(E - E_i) \end{cases}. \quad (3)$$

To prove the validity of the approach, Fiegel et al. [6] examined a model case with three different cross-sections characterized by different threshold energies E_i and Wannier coefficients p_i. Next, the resulting cross-section (3) was fitted by a model function (4):

$$\sigma(E) = A \exp\{p \ln(E - E_1)\}, \quad (4)$$

using a Marquardt-Levenberg algorithm fitting technique. Thus, instead of searching for three partial cross-sections, the single function (4) characterized by a single p and A was used. Such an approach is quite reasonable since in general, the number of single ionic states in the vicinity of the threshold region is unknown. It is worth noting that both fitted magnitudes of p and A were found to be larger than any initial partial p_i and A_i. The smallest E_i of Eq. (3) (i.e., real threshold in the model) and the fitted threshold from Eq. (4) were found to coincide within 25 meV [6].

Similar modeling carried out in the present work confirmed these findings. Based on Eq. (2), the modeling used the same initial partial cross-sections as in ref. [6] and employed the Marquardt-Levenberg algorithm fitting technique. The background level and coefficient A were kept constant, while power p and the threshold magnitude were varied. For a more general scenario whereby all four parameters were varied, the agreement was slightly worse. The thresholds would agree only within 35 meV and, compared to the above mentioned case, the absolute values of the theoretical threshold and p were determined to be of 3.3% lower and 10% higher, respectively.

The electron distribution adds additional complexity to the processing of ionization efficiency curves. The influence of the electron energy spread can be considered in two ways. As applied in ref. [6], the convolution of the fitted cross-section can be considered on the basis of Eqs. (2) or (3), taking the instrumental function (Gaussian) into account. In the present work, another approach has been used which is based on an earlier contribution by Winkler and Märk [17]. An observable ion signal, associated with a separate ion state h, $S_h(E) = C(E - AE)^p$, having an appearance energy AE, is convoluted with the energy spread $G(E, E_0, \Delta E)$ of a real experiment, where E is the electron energy, E_0 is the maximum of the energy distribution, and ΔE is width of the distribution. In the case of m ionic states being superimposed near the threshold, the observed ion signal, $S(E)$, can be written as:

$$S(E) = \sum_{h=1}^{m} \sum_{j=-n}^{n} S_h(E + jdE) \times [G(E, E + jdE, \Delta E)dE]. \quad (5)$$

In contrast to [17], where a fixed exponent p was used, the present work considers the variation of all four parameters (E_i, C, p and background b), applying a weighted non-linear least squares procedure on the basis of the Levenberg-Marquardt algorithm and minimizing:

$$f = \sum_i \{g_i[y_i - S(E_i)\}^2 \to \min, \quad (6)$$

where (E_i, y_i) is the measured data set and a weighting factor g_i is determined by formula (7):

$$g_i = \sqrt{y_i} \sum_i \left(\frac{1}{\sqrt{y_i}}\right), \ \sum g_i \equiv 1. \quad (7)$$

In experiments on the determination of negative ion cross-sections, the apparatus function of the instrument used in the present work, G, was found to be a Voigt function, provided the energy spread is less than 100 meV. The

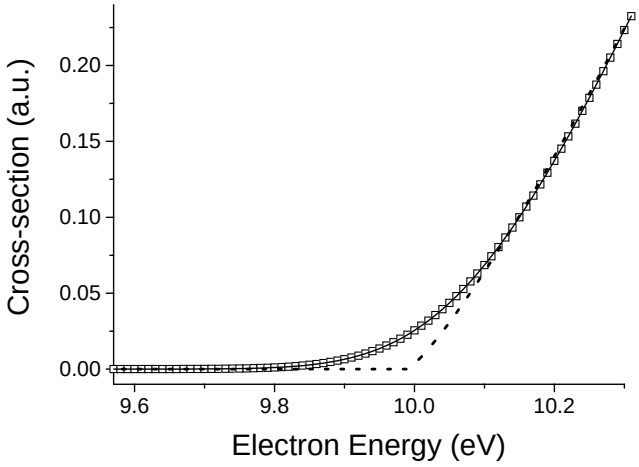

Fig. 1. Results of the convolution of the simulated cross-section ($b = 0$, $c = 1$; $p = 1.13$, $E_1 = 10$ eV) with a Gaussian function, FWHM = 0.3 eV (open squares). The solid curve was obtained by a weighted non-linear fitting of the convoluted data based on Eq. (6). The dotted curve is the result of a similar fitting on the basis of Eq. (2) without taking into account the energy distribution; after convolution with the same Gaussian function, a practically identical behavior to the data of the solid curve is obtained.

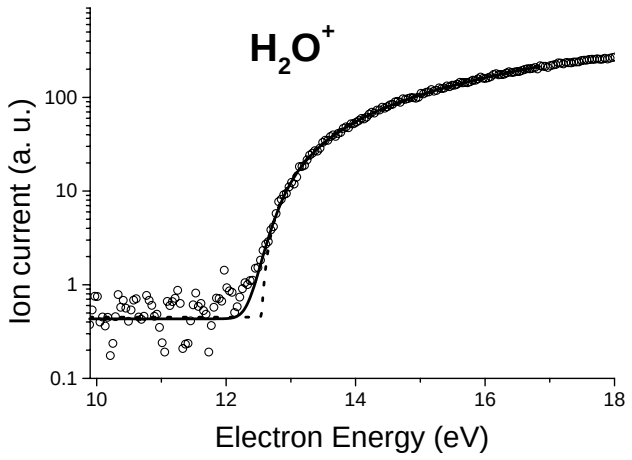

Fig. 2. Experimental ionization efficiency curve of H_2O (open circles). The fitted curves were obtained by the non-linear least squares method with (solid curve—Eq. (6); AE = 12.62±0.01 eV; $p = 1.215 \pm 0.010$) and without (dashed curve—Eq. (2) EA = 12.612 ± 0.011 eV; $p = 1.267 \pm 0.011$) taking into account the energy spread of the electron beam; $E_{high} = 4.2$ eV.

instrument function can be approximated by a Gaussian function if the energy distribution exceeds 100 meV.

To demonstrate the capability of processing the ionization efficiency curve, the method was first applied to handle a result of convolution of a model function (2) ($b = 0$, $c = 1$; $p = 1.13$, $E_1 = 10$ eV) with a Gaussian function, FWHM = 0.3 eV, (Fig. 1). It is of interest to compare the fitting results of the two aforementioned approaches. Fitting on the basis of Eq. (6) resulted in a very good agreement with the original data and the value of $p = 1.131$ is practically equal to the original value. The second method, which applies the convolution procedure to the fitted data separately, also gave good fitting to the original data, but resulted in higher values of $p = 1.21$ and σ (standard deviation).

Similarly to the conclusions drawn by Märk and coworkers [3,5] on the basis of their approach, one can certainly conclude that processing of the raw data on the basis of Eq. (6), as used in the present paper, removes the arbitrariness in the search of the four unknown parameters. The only

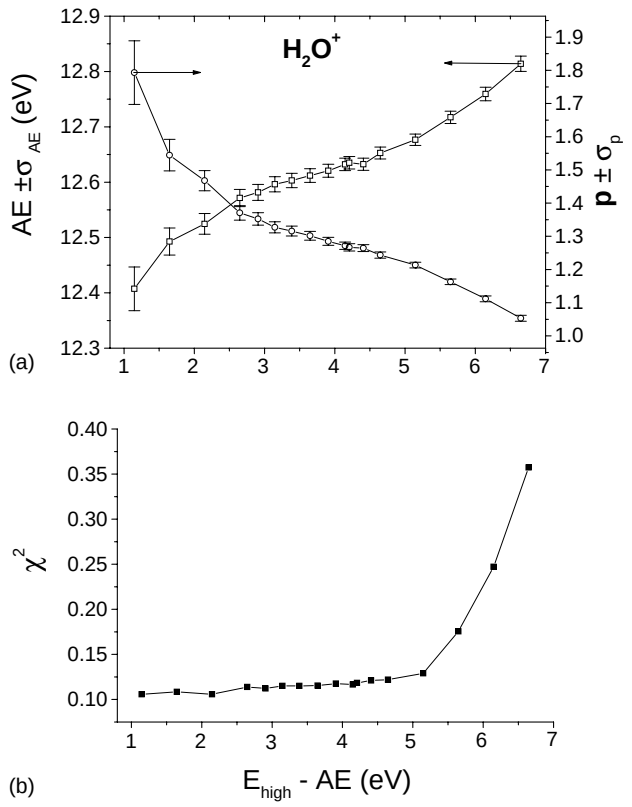

Fig. 3. (a) Values of $E_1 \pm \sigma_{E_1}$ (open squares; left ordinate axis) and p (open circles; right ordinate axis) obtained by fitting the experimental curve in Fig. 2 on the basis of Eq. (6) and constrained vs. E_{high} in the case of the H_2O^+ ion; (b) χ^2 values corresponding to the same fitting procedure and taken as a function of E_{high} for the H_2O^+ ion.

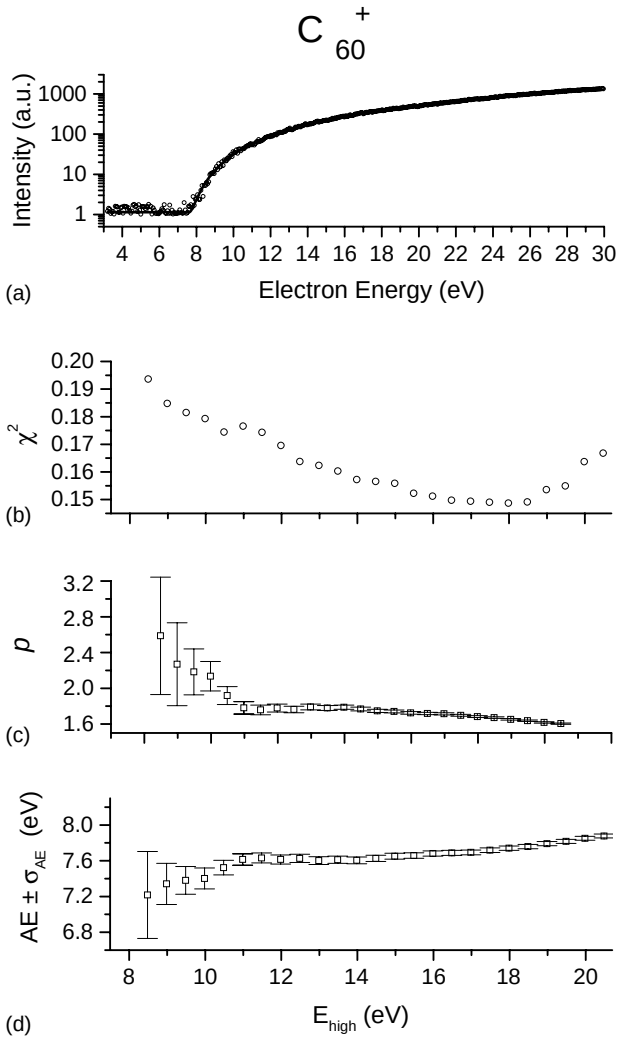

Fig. 4. (a) Ionization efficiency curve of the C_{60}^+ formation (open circles) as a function of electron energy plotted on a semi-logarithmic scale (for clarity of the presentation, only every fourth experimental point is shown); solid curve is the fitted curve obtained by the non-linear least squares method on the basis of Eq. (6); (b) values of χ^2 vs. E_{high}; values of exponents p; (c) and $E_1 \pm \sigma_{E_1}$ (d) vs. E_{high} both obtained by fitting the experimental curve of C_{60}^+ on the basis of Eq. (6).

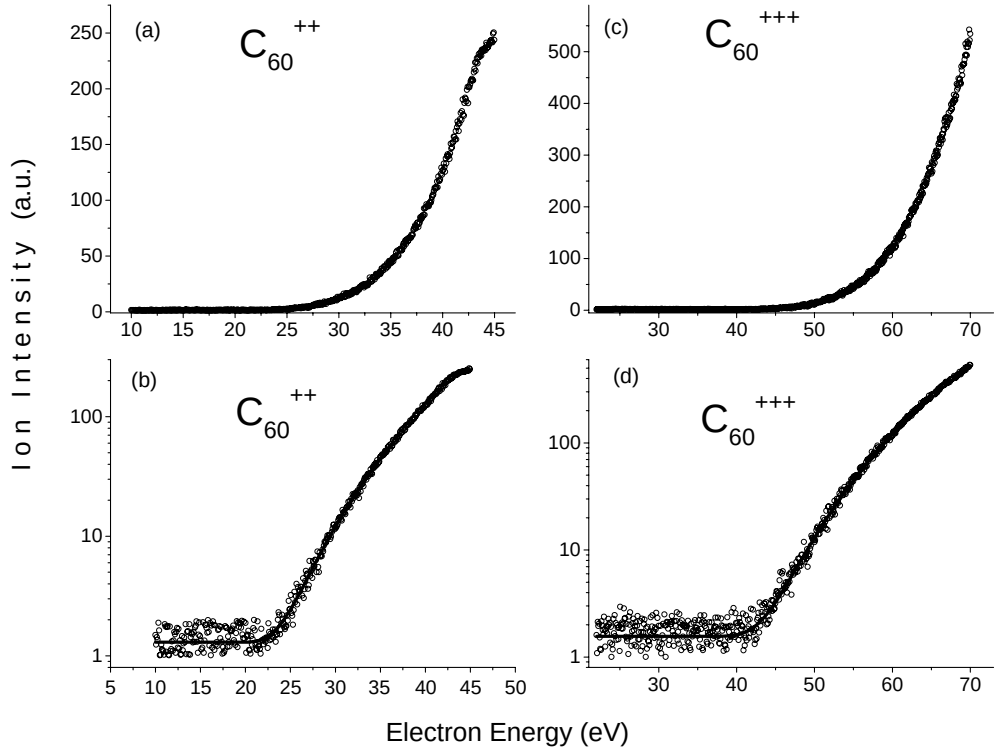

Fig. 5. (a) Ionization efficiency curve of the C_{60}^{2+} formation (open circles) as a function of electron energy plotted on a linear scale (for clarity of the presentation, only every fourth experimental point is shown); (b) the same as (a) plotted on a semi-logarithmic scale (open circles) including the fitted curve (solid curve) obtained by the non-linear least squares method on the basis of Eq. (6) (only every fourth experimental point is shown); (c) ionization efficiency curve of the C_{60}^{3+} formation (open circles) as a function of electron energy plotted on a linear scale (only every fourth experimental point is shown); (d) the same as (c) plotted on a semi-logarithmic scale (open circles) including the fitted curve (solid curve) obtained by the non-linear least squares method on the basis of Eq. (6) (only every fourth experimental point is shown).

exception is the choice of an energy range [E_{low}, E_{high}] over which the non-linear fit is executed. In complete agreement with refs. [3] and [5], it was found that the choice of E_{low} is not crucial if it is well below E_1 and if the background is constant. The value of E_{high} has, however, a pronounced effect on the results. The present fitting procedure demonstrated that higher values of E_{high} tend to produce larger values of E_1 and smaller values of p with small statistical errors, σ. Smaller values of E_{high} result in smaller values of E_1 and larger p combined with large uncertainties, σ. Figs. 2 and 3 clearly indicate these findings for the case of positive H_2O^+ ions. In this respect, these findings differ from those of Märk and coworkers [3,5], who found that high values of E_{high} lead to the enlargement of both E_1 and p at small errors σ, while low E_{high} values result in smaller values of E_1 and p combined with a large σ. The peculiarity of the present fitting procedure to produce lower values of p, is certainly an advantage of the method, as lower values are closer to the Wannier exponent [1].

Fig. 3a clearly shows that there is a range of E_{high} over which the theoretical threshold E_1 (EA in the figure) is approximately constant, so that the derivative of E_1 with respect to E_{high} is insignificant. Therefore, E_1 can be chosen as a mean over this range of E_{high}. E_1 values can be rejected at larger E_{high} values, because the χ^2 values become very large (Fig. 3b), signifying the bad quality of the model. The quality of the fitting procedure can be checked by comparison of the H_2O ionization energy determined in the present work (12.62 ± 0.01 eV) with the recommended value (12.612 ± 0.010) [18]. Finally, it is worth noting that at low signal-to-noise ratio, the dependence of E_1 upon E_{high} is not always monotonic. Nevertheless, even in these cases it is still possible to distinguish the range of E_1 values that are approximately constant, allowing the averaging of E_1 in this region. Another important point concerns the display of χ^2 values versus E_{high}, which, unlike the situation shown in Fig. 3b, very often results in a minimum, corresponding to the optimal value of E_{high}.

4. Results and discussion

The method described in the previous section has been applied to the processing of the ionization efficiency curves of singly-, doubly-, and triply-charged positive fullerene ions. The raw data of C_{60}^{+}, C_{60}^{2+} and C_{60}^{3+} are shown in Figs. 4 and 5, together with the theoretical images obtained by the fitting procedure. The resulting data and the comparison with the literature data are presented in

Table 1
Appearance energies of the positively-charged molecular ions of the compounds under investigation and the exponential factor of the power law

Ions	Present work		Literature data AE (eV) [reference]
	AE (eV)	Exponent	
C_{60}^+	7.65 ± 0.20	1.89 ± 0.05	$7.58^{+0.04}_{-0.02}$ [19]; 7.64 ± 0.02 [20]
C_{60}^{2+}	18.98 ± 0.25	3.7 ± 0.1	19.0 ± 0.5 [4]
C_{60}^{3+}	35.8 ± 0.3	4.4 ± 0.1	35.6 ± 1 [4]
$C_{60}H_{36}^+$	7.01 ± 0.25	1.59 ± 0.02	–
$C_{60}H_{18}^+$	7.3 ± 0.3	1.36 ± 0.05	–
$C_{60}H_{36}^{2+}$	18.7 ± 0.2	2.50 ± 0.06	–

Table 1. The errors given in Table 1 are mostly statistical errors and for enhanced ion abundances, the errors could be much less, because the energy resolution of the monochromator is lower than these statistical uncertainties. But even in this case, the agreement of the present results with the most reliable literature data is indeed satisfactory.

According to theoretical predictions for hydrogenated fullerenes [21], the ionization energies of these compounds should be lower than for the pure C_{60} molecule. As mentioned earlier, Compton and coworkers [9] provided a tentative hint that this tendency indeed exists. Nevertheless, up to now there has been no experimental determination of the appearance energies for the molecular ions of the two most prominent hydrofullerene representatives, $C_{60}H_{18}$ and $C_{60}H_{36}$. The ionization efficiency curves for these ions are depicted in Figs. 6 and 7 (see also Table 1), together with the details of the fitting procedure. The figures clearly indicate that there is indeed quantitative agreement with the aforementioned theoretical prediction [21] of lower ionization energies of the hydrogenated fullerenes. The data also reveal a slightly higher ionization energy of $C_{60}H_{18}$ compared with $C_{60}H_{36}$. This finding seems to contradict recently reported calculations of the most stable isomers of $C_{60}H_{2x}$ (x = 1–30) with three-fold symmetry axes [22], showing a lower value for $C_{60}H_{18}$. However, a direct comparison of these values is probably not as straightforward. There exists at least two isolated isomers of $C_{60}H_{36}$ of C_3 and T symmetry [23], which may possess different ionization energies. Therefore, depending on the experimental conditions, the isomers may contribute quite differently towards the measured ion signal. Based on our negative ion experiments with $C_{60}F_{18}^-$ (unpublished) and $C_{60}H(D)_{18}^-$ [24] we would assume that there exists at least one more stable isomer for these molecules in addition to the well established C_{3v} geometry [25]. As a consequence, the measured ionization energies of $C_{60}H_{18}$ and $C_{60}H_{36}$ may well be influenced by a collective effect caused by several isomers, so that the comparison with only the most stable isomer [22] may not be justified.

Finally, the appearance energy of $C_{60}H_{36}^{2+}$ has been measured as well (Fig. 8; Table 1). Although the appearance energy of $C_{60}H_{36}^{2+}$ is lower than that of C_{60}^{2+}, the second ionization energy of the hydrogenated fullerene (11.69 ± 0.3 eV; determined as the difference of the appearance energies of $C_{60}H_{36}^+$ and $C_{60}H_{36}^{2+}$) has been found to be slightly larger than that of C_{60} (11.3 ± 0.4 eV). Efforts to determine the energetics of the $C_{60}H_{18}^{2+}$ formation were unsuccessful in the present experiments for the following reasons. First, it was impossible to achieve a high enough density of $C_{60}H_{18}$ vapor in the ionization

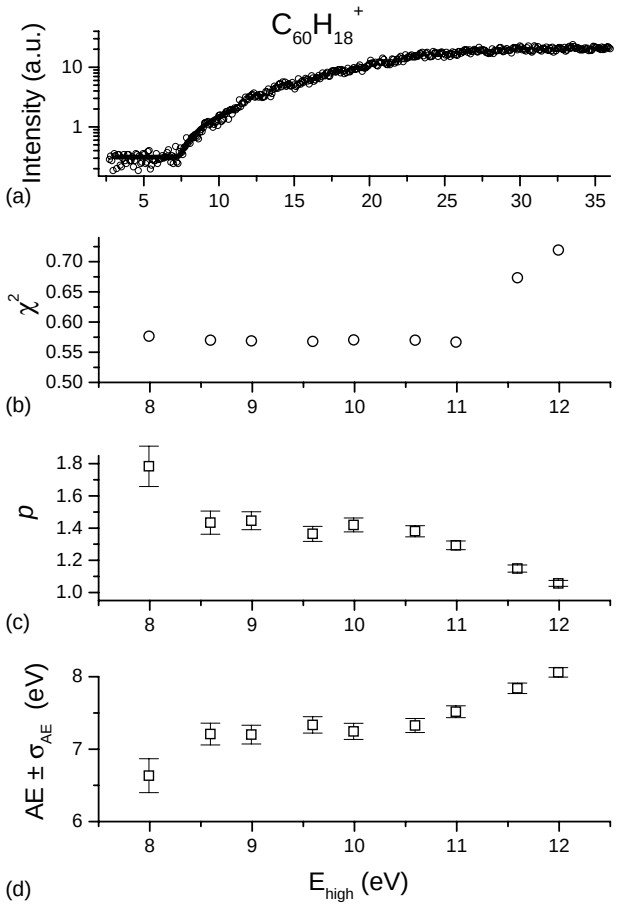

Fig. 6. (a) Ionization efficiency curve of the $C_{60}H_{18}^+$ formation (open circles) as a function of electron energy plotted on a semi-logarithmic scale (for clarity of the presentation, only every fourth experimental point is shown); solid curve is the fitted curve obtained by the non-linear least squares method on the basis of Eq. (6); (b) values of χ^2 vs. E_{high}; (c) values of exponents p and (d) $E_1 \pm \sigma_{E_1}$ vs. E_{high} both obtained by fitting the experimental curve of $C_{60}H_{18}^+$ on the basis of Eq. (6).

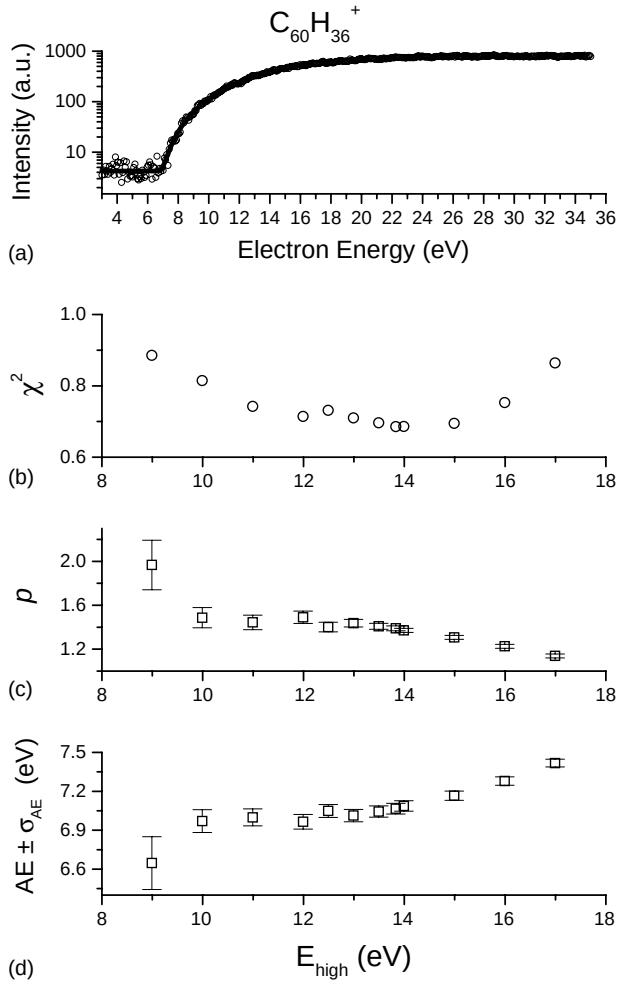

Fig. 7. (a) Ionization efficiency curve of the $C_{60}H_{36}^{+}$ formation (open circles) as a function of electron energy plotted on a semi-logarithmic scale (for clarity of the presentation, only every fourth experimental point is shown); solid curve is the fitted curve obtained by the non-linear least squares method on the basis of Eq. (6); (b) values of χ^2 vs. E_{high}; (c) values of exponents p; and (d) $E_1 \pm \sigma_{E_1}$ vs. E_{high} both obtained by fitting the experimental curve of $C_{60}H_{36}^{+}$ on the basis of Eq. (6).

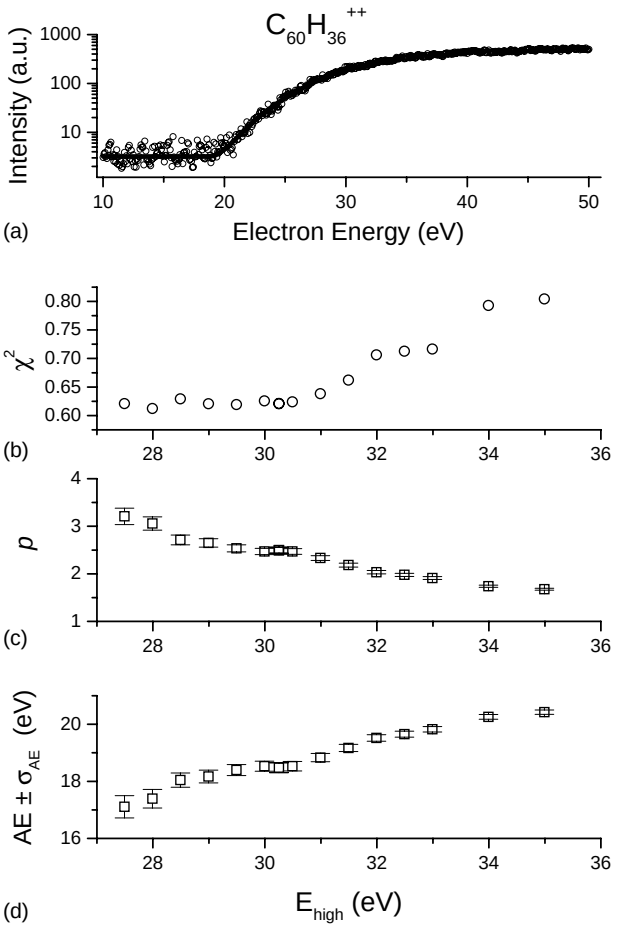

Fig. 8. (a) Ionization efficiency curve of the $C_{60}H_{36}^{2+}$ formation (open circles) as a function of electron energy plotted on a semi-logarithmic scale (for clarity of the presentation, only every fourth experimental point is shown); solid curve is the fitted curve obtained by the non-linear least squares method on the basis of Eq. (6); (b) values of χ^2 vs. E_{high}; values of exponents p (c) and (d) $E_1 \pm \sigma_{E_1}$ vs. E_{high} both obtained by fitting the experimental curve of $C_{60}H_{36}^{2+}$ on the basis of Eq. (6).

chamber, because compared to $C_{60}H_{36}$ this sample needed a higher temperature for the evaporation (see Section 2), which in turn facilitated the decomposition of $C_{60}H_{18}$. As a result, the signal of $C_{60}H_{18}^{+}$ (Fig. 6) was much weaker with respect to that of $C_{60}H_{36}^{+}$ (Fig. 7). Consequently, the $C_{60}H_{18}^{2+}$ ion signal was also weak and did not markedly exceed the background level which typically increases towards lower masses. In the present experiments, it was not possible to reduce the background level at the nominal mass of $C_{60}H_{18}^{2+}$ as to allow the unambiguous recording of its ionization efficiency curve. The same problem was encountered for $C_{60}H_{18}^{3+}$ and $C_{60}H_{36}^{3+}$, although both these ions were clearly present in mass spectra when recorded at a fixed electron energy of 80 eV. It is hoped that in the future one can overcome these technical problems in order to measure the corresponding ionization energies.

5. Conclusion

A modification is presented of a method initially developed by Märk and coworkers for the processing of ionization efficiency curves of polyatomic molecules, as used for the determination of ionization energies by electron ionization. The new method is based on the minimization of differences between the experimental raw data and a theoretical curve convoluted with an instrumental function and obtained by a weighted non-linear fitting procedure. The method has been checked by handling a known model function and in comparison with tabulated data on C_{60}^{+}, C_{60}^{2+}, and C_{60}^{3+}. The main advantage of the method is the ability to produce reliable appearance energies combined with lower values of the effective Wannier coefficients of the fitted theoretical curves. Next, the ionization energies of hydrogenated fullerenes $C_{60}H_{18}$ and $C_{60}H_{36}$ have been determined on the basis of this method. It was found that the single ionization energies

of the hydrogenated fullerenes $C_{60}H_{18}$ and $C_{60}H_{36}$ are both lower in value with respect to that of pure C_{60}, which is in line with earlier theoretical predictions. The second ionization energy of $C_{60}H_{36}$ has been found to be higher than that of C_{60} although the appearance energy of $C_{60}H_{36}^{2+}$ has been determined to be lower than that of C_{60}^{2+}. The present experiments were unsuccessful in measuring the second ionization energy of $C_{60}H_{18}$ due to its weak molecular density in the present experiments and because of background interferences. Future work will focus on further improvements of the experimental setup in order to measure the second ionization energy of $C_{60}H_{18}$ and the third ionization energies of both hydrogenated fullerenes under investigation.

Acknowledgements

Y.V.V. acknowledges the invaluable support by Professor Max L. Deinzer (NIH (USA) ES-00210 and RO1 ES9536). Furthermore, Y.V.V. would like to thank Professor Paul Scheier for many helpful discussions during a recent conference in Lincoln (USA) and Gernot Hanel for sending his Diploma thesis. This work was partly supported by the Russian Foundation for Basic Research (grant 01-02-16561) and by the Leverhulme Trust (UK).

References

[1] G.H. Wannier, Phys. Rev. 90 (1953) 817.
[2] R. Wörgötter, B. Dünser, P. Scheier, T.D. Märk, J. Chem. Phys. 101 (1994) 8674.
[3] S. Matt, O. Echt, R. Wörgötter, V. Grill, P. Scheier, C. Lifschitz, T.D. Märk, Chem. Phys. Lett. 264 (1997) 149.
[4] P. Scheier, B. Dünser, R. Wörgötter, M. Lezius, R. Robl, T.D. Märk, Int. J. Mass Spectrom. Ion Proc. 138 (1994) 77.
[5] D. Muigg, G. Denifl, A. Stamatovic, O. Echt, T.D. Märk, Chem. Phys. 239 (1998) 409.
[6] T. Fiegele, G. Hanel, I. Torres, M. Lezius, T.D. Märk, J. Phys. B: At. Mol. Opt. Phys. 33 (2000) 4263.
[7] Y.V. Vasil'ev, O.V. Boltalina, R.F. Tuktarov, V.A. Mazunov, L.N. Sidorov, Int. J. Mass Spectrom. Ion Proc. 173 (1998) 113.
[8] H. Steger, U. Mische, W. Kamke, A. Ding, M. Fieber-Erdmann, T. Drewello, Chem. Phys. Lett. 276 (1997) 39.
[9] C. Jin, R. Hettich, R. Compton, D. Joyce, J. Blencoe, T. Burch, J. Phys. Chem. 98 (1994) 4215.
[10] Y.V. Vasil'ev, R.F. Tuktarov, V.A. Mazunov, Rapid Commun. Mass Specrom. 11 (1997) 757.
[11] M.V. Muftakhov, Y.V. Vasil'ev, E.R. Nazirov, M.A. Mazunov, Pribory I Tekhnika Eksperimenta 2 (1989) 166 (in Russian) (in English translation: Sov. Instruments and Experimental Techniques).
[12] A. Stamatovic, G.J. Schulz, Rev. Sci. Instrum. 39 (1968) 1752; A. Stamatovic, G.J. Schulz, Rev. Sci. Instrum. 41 (1970) 423.
[13] N.F. Goldshleger, A.P. Moravsky, Russ. Chem. Rev. 66 (1997) 323.
[14] C. Rückhardt, M. Gerst, J. Ebenhoch, H.-D. Beckhaus, E.E.B. Campbell, R. Tellgmann, H. Schwarz, T. Weiske, S. Pitter, Angew. Chem. Int. Ed. Engl. 32 (1993) 584.
[15] A.S. Lobach, A.A. Perov, A.I. Rebrov, O.S. Roshchupkina, V.A. Tkacheva, A.N. Stepanov, Russ. Chem. Bull. 46 (1997) 641.
[16] Y. Vasil'ev, D. Wallis, M. Nüchter, B. Ondruschka, A. Lobach, T. Drewello, Chem. Commun. (2000) 1233.
[17] C. Winkler, T.D. Märk, Int. J. Mass Spectrom. Ion Proc. 133 (1994) 157.
[18] M.W. Chase, Jr., C.A. Davies, J.R. Downey, Jr., D.J. Frurip, R.A. McDonald, A.N. Syverud, "JANAF Thermochemical Tables (3rd Edition) Suppl. 1", J. Phys. Chem. Ref. Data 14 (1985).
[19] J. de Vries, H. Steger, B. Kamke, C. Menzel, B. Weisser, W. Kamke, I.V. Hertel, Chem. Phys. Lett. 188 (1992) 159.
[20] D.L. Lichtenberg, M.E. Jatcko, K.W. Nebesny, C.D. Ray, D.R. Huffmann, L.D. Lamb, Chem. Phys. Lett. 198 (1992) 454.
[21] N. Matsuzawa, T. Fukunaga, D.A. Dixon, J. Phys. Chem. 96 (1992) 10747.
[22] S.K. Nasibullaev, G.D. Davletbaeva, Y.V. Vasil'ev, I.S. Nasibullayev, Fullerene, Nanotubes Carbon Nanostruct. 12 (2004) 513.
[23] O.V. Boltalina, M. Bühl, A. Khong, M.A. Saunders, J. Street, R. Taylor, J. Chem. Soc., Perkin Trans. 2 (1999) 1475.
[24] S.K. Nasibullaev, Y.V. Vasil'ev, R.R. Abzalimov, A.S. Lobach, I.O. Bashkin, D. Wallis, T. Drewello, Phys. Solid State 44 (2002) 551.
[25] I.S. Neretin, K.A. Lyssenko, M.Yu. Antipin, Y.L. Slovokhotov, O.V. Boltalina, P.A. Troshin, A.Yu. Lukonin, L.N. Sidorov, R. Taylor, Angew. Chem. Int. Ed. 39 (2000) 3273.